A hippocampal interneuron associated with the mossy fiber system

Imre Vida and Michael Frotscher*

Anatomisches Institut, Albert-Ludwigs-Universität Freiburg, D-79104 Freiburg, Germany

Edited by Per O. Andersen, University of Oslo, Oslo, Norway, and approved November 3, 1999 (received for review July 8, 1999)

Network properties of the hippocampus emerge from the interaction of principal cells and a heterogeneous population of interneurons expressing γ-aminobutyric acid (GABA). To understand these interactions, the synaptic connections of different types of interneurons need to be elucidated. Here we describe a type of inhibitory interneuron of the hippocampal CA3 region that has an axon coaligned with the mossy fibers. Whole-cell patch-clamp recordings, in combination with intracellular biocytin filling, were made from nonpyramidal cells of the stratum lucidum under visual control. Mossy fiber-associated (MFA) interneurons generated brief action potentials followed by a prominent after-hyperpolarization. Subsequent visualization revealed an extensive axonal arbor which was preferentially located in the stratum lucidum of CA3 and often invaded the hilus. The dendrites of MFA interneurons were mainly located in the strata radiatum and oriens, suggesting that these cells are primarily activated by associational and commissural fibers. Electron microscopic analysis showed that axon terminals of MFA interneurons established symmetric synaptic contacts predominantly on proximal apical dendritic shafts, and to a lesser degree, on somata of pyramidal cells. Synaptic contacts were also found on GABAergic interneurons of the CA3 region and putative mossy cells of the hilus. Inhibitory postsynaptic currents (IPSCs) elicited by MFA interneurons in simultaneously recorded pyramidal cells had fast kinetics (half duration, 3.6 ms) and were blocked by the $GABA_A$ receptor antagonist bicuculline. Thus, MFA interneurons are GABAergic cells in a position to selectively suppress the mossy fiber input, an important requirement for the recall of memory traces from the CA3 network.

The hippocampus is essential for the formation of conscious memories (1, 2). Although its exact role in learning and memory processes is not yet established (2), several theories suggest that memory traces are initially stored in the hippocampus and subsequently transferred to neocortical areas (3–5). Within the hippocampus, the CA3 region is unique because of its abundant recurrent excitatory connections (6) and may act as an attractor network (7) to form associations of neuronal representations instantaneously (5, 8, 9).

Circuits of the hippocampus involve principal cells and a heterogeneous population of interneurons (10). Interneurons give rise to an extensive local axonal arbor affecting the activity of large populations of neurons. Their axons show a laminar distribution paralleled by a domain-specific innervation of the target cells (11–15). The wide variety of interneurons most conceivably reflects a division of labor among the different types, allowing for fine tuning of the activity of the population (13, 16). Indeed, several types of interneurons express distinct sets of ligand- and voltage-gated ion channels (17–19) and respond differently to activation (10, 15, 20). Furthermore, inhibition itself has a differential effect on the activity of target neurons depending on the postsynaptic compartment involved (21–23). In addition to these postsynaptic influences, interactions between excitatory and inhibitory circuits may also exist presynaptically. γ-Aminobutyric acid (GABA) released from the axons of interneurons can diffuse to excitatory terminals and decrease the probability of glutamate release via presynaptic $GABA_B$ receptors (24). Because several types of interneurons display a coalignment of their axon with defined afferent fiber systems (11, 25), such a mechanism could provide a basis for the selective modulation of the laminated inputs by similarly laminated inhibitory circuits.

The majority of intracellular labeling studies so far were done "blind," thus sampling mainly regions enriched in GABAergic neurons. By using whole-cell patch-clamp recordings and infrared videomicroscopy in combination with biocytin labeling, we describe here a type of GABAergic interneuron in the stratum lucidum of the CA3 region with an axon associated with the mossy fibers. Besides electrophysiological and morphological properties, we analyze their postsynaptic targets and characterize their postsynaptic effects in simultaneously recorded pyramidal cells.

Materials and Methods

Whole-cell patch-clamp recordings from nonpyramidal neurons in the stratum lucidum of CA3 in hippocampal slices were made under visual control by infrared differential interference contrast videomicroscopy (26). Slices (300–400 μm) were prepared from 16- to 19-day-old Wistar rats by using a vibratome (Dosaka Instruments, Kyoto). The artificial cerebrospinal fluid used for bath perfusion was composed of: 125 mM NaCl, 25 mM $NaHCO_3$, 25 mM glucose, 2.5 mM KCl, 1.25 mM NaH_2PO_4, 2 mM $CaCl_2$, and 1 mM $MgCl_2$, and was bubbled with 95% O_2 and 5% CO_2. Patch pipettes pulled from borosilicate glass tubing (2.0/1.0 mm o.d./i.d., Hilgenberg, Malsfeld, Germany) had a resistance of 1–3 MΩ when filled with internal pipette solution containing (*i*) 135 mM potassium gluconate, 20 mM KCl, 0.1 mM EGTA, 10 mM Hepes, 2 mM $MgCl_2$, and 2 mM ATP (disodium salt) for recording interneurons, or (*ii*) 78 mM potassium gluconate, 78 mM KCl, 0.1 mM EGTA, 10 mM Hepes, 2 mM $MgCl_2$, and 2 mM ATP for pyramidal cells, with 1–5 mg/ml biocytin added to both solutions. All recordings from mossy fiber-associated (MFA) interneurons were performed in the fast current-clamp mode of an Axopatch 200B amplifier (Axon Instruments, Foster City, CA) at a temperature of 32–34°C; pyramidal cells were recorded in the voltage-clamp mode by using whole-cell capacitance and series resistance compensation (80–90%). To elicit unitary inhibitory postsynaptic currents (IPSCs), action potentials (APs) were evoked in the MFA interneurons by 2 ms suprathreshold current pulses; traces were collected at a rate of 0.33 s^{-1}.

Recordings were filtered at 2–5 kHz and digitized at 5–10 kHz. Data analysis was performed off-line by using custom-made software (courtesy of P. Jonas, University of Freiburg, Germany). The input resistance and apparent membrane time constant were determined from responses to hyperpolarizing current pulses (200 ms, −10 or −20 pA). The amplitude of APs was

This paper was submitted directly (Track II) to the PNAS office.

Abbreviations: GABA, γ-aminobutyric acid; IPSCs, inhibitory postsynaptic currents; MFA, mossy fiber-associated; AP, action potential; AHP, after-hyperpolarization.

*To whom reprint requests should be addressed. E-mail: frotsch@uni-freiburg.de.

The publication costs of this article were defrayed in part by page charge payment. This article must therefore be hereby marked "*advertisement*" in accordance with 18 U.S.C. §1734 solely to indicate this fact.

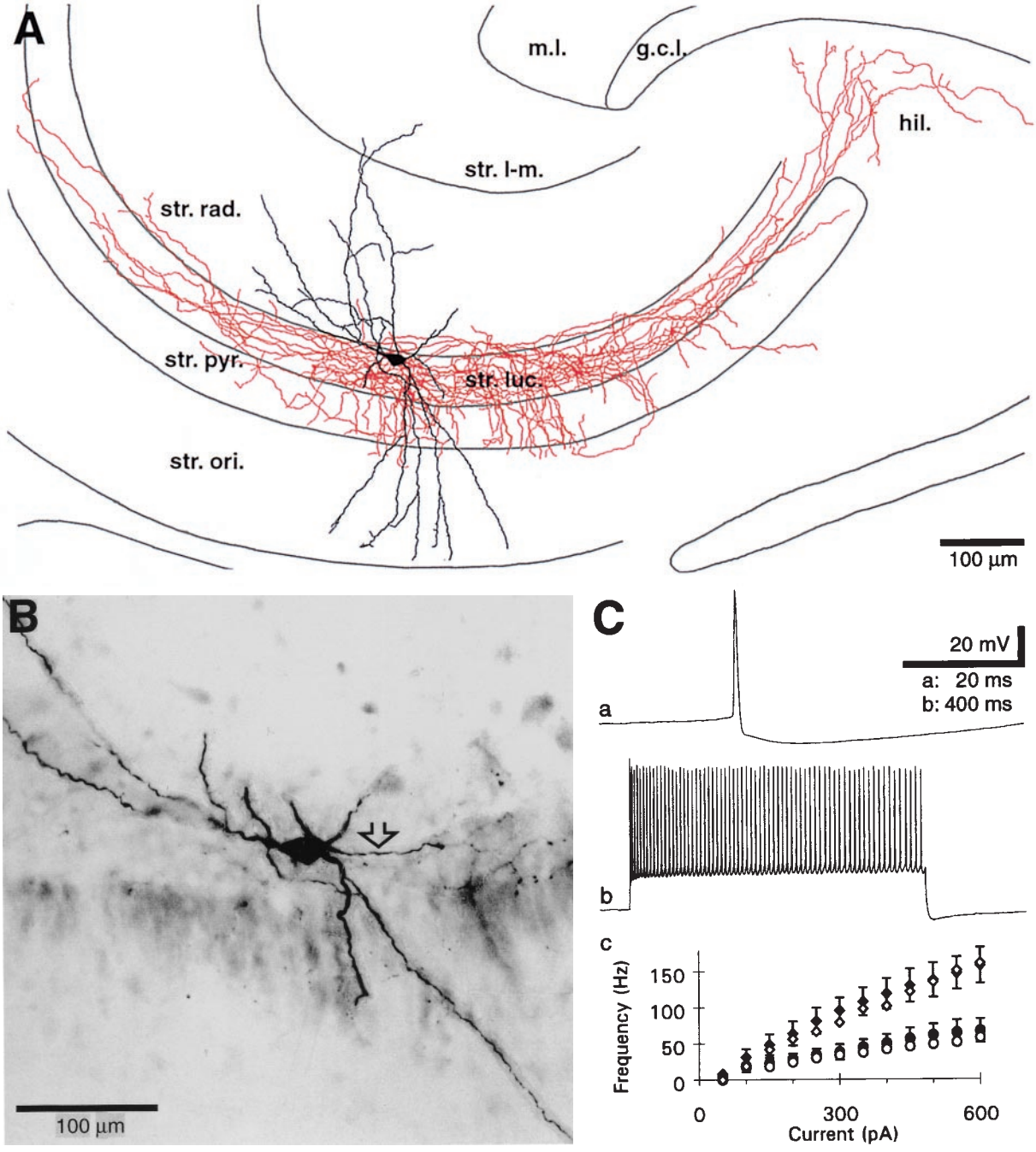

Fig. 1. An MFA interneuron in the stratum lucidum of the hippocampal CA3 region. (*A*) Camera lucida reconstruction of the biocytin-filled interneuron. The soma and dendrites are drawn in black, whereas the axon is in red; hippocampal layers are depicted schematically. str. ori., stratum oriens; str. pyr., stratum pyramidale; str. luc., stratum lucidum; str. rad., stratum radiatum; str. l.-m., stratum lacunosum-moleculare; m.l., molecular layer of the dentate gyrus; g.c.l., granule cell layer of the dentate gyrus; and hil., hilar region. (*B*) Photomontage from a section of the slice containing the soma of the interneuron. The axon emerging from the soma is indicated by an arrow. (*Ca*) APs of brief duration were followed by large amplitude biphasic AHPs in the interneuron. (*Cb*) A train of APs elicited by a suprathreshold current pulse (500 pA) displays spike frequency adaptation. (*Cc*) Initial (◆) and steady-state firing frequencies (●) of trains of APs elicited in MFA interneurons ($n = 13$) by depolarizing current pulses plotted against the amplitude of the pulses. Error bars indicate SD; ◇ and ○ represent the respective values for the interneuron shown in *A*.

taken from baseline; amplitude of after-hyperpolarizations (AHPs) was measured from the inflection point of the APs. The duration of APs and AHPs was measured at half amplitude. Maximum firing frequency was taken as the number of APs in response to a 1-s suprathreshold current pulse (400–600 pA). Latency of unitary IPSCs was taken as the interval between the maximum of the first derivative of the presynaptic APs and the beginning of the IPSCs. Kinetic parameters of the IPSCs were determined in averaged responses aligned on their rising phase.

Following immersion fixation (1% paraformaldehyde and 2.5% glutaraldehyde in 0.1 M phosphate buffer), biocytin-labeled neurons were developed by using avidin-biotinylated

Table 1. Electrophysiological properties of MFA interneurons and type I (fast spiking) and type II interneurons of the CA3 stratum lucidum

	MFA ($n = 13$)	Type I (fast spiking) ($n = 3$)	Type II ($n = 27$)
Resting membrane potential, mV	−57 ± 5	−53 ± 1*	−56 ± 6
	−51, −69	−52, −54	−50, −71
Input resistance, MΩ	225 ± 93	154 ± 103	281 ± 106
	132, 443	71, 270	124, 504
Apparent membrane time constant, ms	29.1 ± 14.6	13.8 ± 8.3	38.5 ± 24.8
	12.7, 61.3	8.2, 23.3	10.6, 117.0
Maximum discharge frequency, s^{-1}	73 ± 16	203 ± 18**	69 ± 21
	48, 101	187, 222	37, 123
Action potential amplitude, mV	94 ± 8	83 ± 14	91 ± 8
	83, 110	73, 99	76, 104
Action potential duration, ms	0.72 ± 0.15	0.35 ± 0.04**	0.82 ± 0.27
	0.58, 1.16	0.32, 0.40	0.44, 1.37
AHP amplitude, mV	−13.1 ± 1.9	−17.6 ± 2.1*	−14.2 ± 3.9
	−9.9, −16.0	−16.4, −20.1	−8.7, −19.9
AHP duration, ms	57.2 ± 18.1	8.2 ± 2.5**	48.6 ± 11.9
	34.9, 84.5	5.4, 10.0	27.0, 69.3

For each parameter, the mean ± SD and range are given. Asterisks indicate values significantly different from those of MFA interneurons: *, $P < 0.05$; **, $P < 0.01$.

horseradish peroxidase complex (ABC, Vector Laboratories) and 3,3′-diaminobenzidine tetrahydrochloride as a chromogen (25). Representative neurons were photographed and reconstructed with the aid of a camera lucida at a final magnification of ×762; the length of the axons was measured with a curvimeter. Following light microscopic analysis, areas of interest were reembedded, sectioned serially, and examined with an electron microscope. Immunogold staining followed the procedure described by Somogyi and Hodgson (27) with use of a commercially available rabbit antiserum against GABA (Sigma; diluted 1:5000 in Tris-buffered saline). In control experiments without the primary antibody, no immunogold labeling was detected.

All values are given as the mean ± SD unless otherwise noted. For statistical comparison, the Student's unpaired *t* test and the χ^2 test were used. Bicuculline methochloride was obtained from Tocris Neuramin (Bristol, U.K.); all other chemicals were from Merck or Sigma.

Results

Eighteen out of 64 recorded and biocytin-labeled interneurons (28%) displayed a previously undescribed preferential termination in the stratum lucidum, coaligned with the mossy fibers (Fig. 1 *A* and *B*). Having largely similar physiological and morphological features, these nonpyramidal cells were grouped together and named MFA interneurons.

During recordings, MFA neurons generated brief APs followed by a prominent AHP characteristic of interneurons (Fig. 1*Ca*). In response to large depolarizing current pulses, the cells discharged at high frequencies but showed strong spike frequency adaptation (Fig. 1 *Cb* and *Cc*). When compared with interneurons with the typical "fast-spiking" firing pattern (type I interneurons, ref. 20), significant differences were found in several intrinsic electrophysiological parameters such as maximal firing frequency, duration of the AP, and the AHP (Table 1). Despite these differences, however, MFA interneurons were not identifiable by electrophysiological properties alone because most other interneurons recorded in the stratum lucidum showed very similar properties (type II interneurons, ref. 20; Table 1).

All MFA interneurons had extensive axonal arbors that were primarily located in the stratum lucidum of the CA3 region (Fig. 1*A*). Axon collaterals also entered the pyramidal layer, often reaching the border of the stratum oriens. In the stratum radiatum, axon collaterals were found only in the region adjacent to the stratum lucidum, and no collaterals were found in the stratum lacunosum-moleculare. Axon collaterals in the stratum lucidum had a preferential horizontal orientation, whereas those in the pyramidal layer mainly ran vertically (Fig. 1*A*). The axonal arbor covered 50–100% of the total extent of the CA3 region in these transverse slices of the hippocampus, often extending into the adjacent hilus ($n = 7$; Fig. 1*A*). For a quantitative estimation of the axonal distribution of MFA interneurons, three representative cells were reconstructed. The mean total axonal length was 24.5 mm (range: 20.3–28.6 mm). On average, 69.8% (65.3–73.0%) of the axons remaining within the CA3 region were located in the stratum lucidum, 25.6% (19.4–33.0%) in the pyramidal layer and the adjacent zone of stratum oriens, and only 4.6% (1.7–7.6%) were found in stratum radiatum. Two of these cells (Fig. 1*A*) had significant portions of their axons terminating in the hilar region (12.7% and 10.5% of the total length, respectively). Axon collaterals formed boutons of variable size at approximately equal distances along their course. The average distance between boutons was between 4.0 and 4.3 μm. On the basis of the total axonal length and the mean interbouton distance, we estimated the number of boutons to be in the range of 5,000–7,000.

Dendrites of MFA interneurons had a beaded appearance and were generally smooth, although in four interneurons, a few spines were found. The dendrites were mainly located in the stratum radiatum and stratum oriens (Fig. 1*A*). None of these interneurons had a significant number of dendrites in the stratum lacunosum-moleculare.

To determine the postsynaptic targets of MFA interneurons, a total of 90 synaptic contacts was analyzed in serial thin sections from four neurons ($n = 16$–34 synapses per cell). The postsynaptic densities of these synapses were all thin, indicating symmetric contacts (Fig. 2). The majority of the synaptic contacts in the CA3 area ($n = 72$ out of 85; 84.7%) were located on dendritic shafts (Fig. 2 *A–C*), whereas the remaining 15.3% were on somata (Fig. 2*D*). Most postsynaptic shafts were identified as proximal dendrites of CA3 pyramidal neurons by the presence of large spines originating from these dendrites which formed synapses with characteristic large mossy-fiber boutons (Fig. 2*A*). MFA axon terminals also established contacts with GABAergic

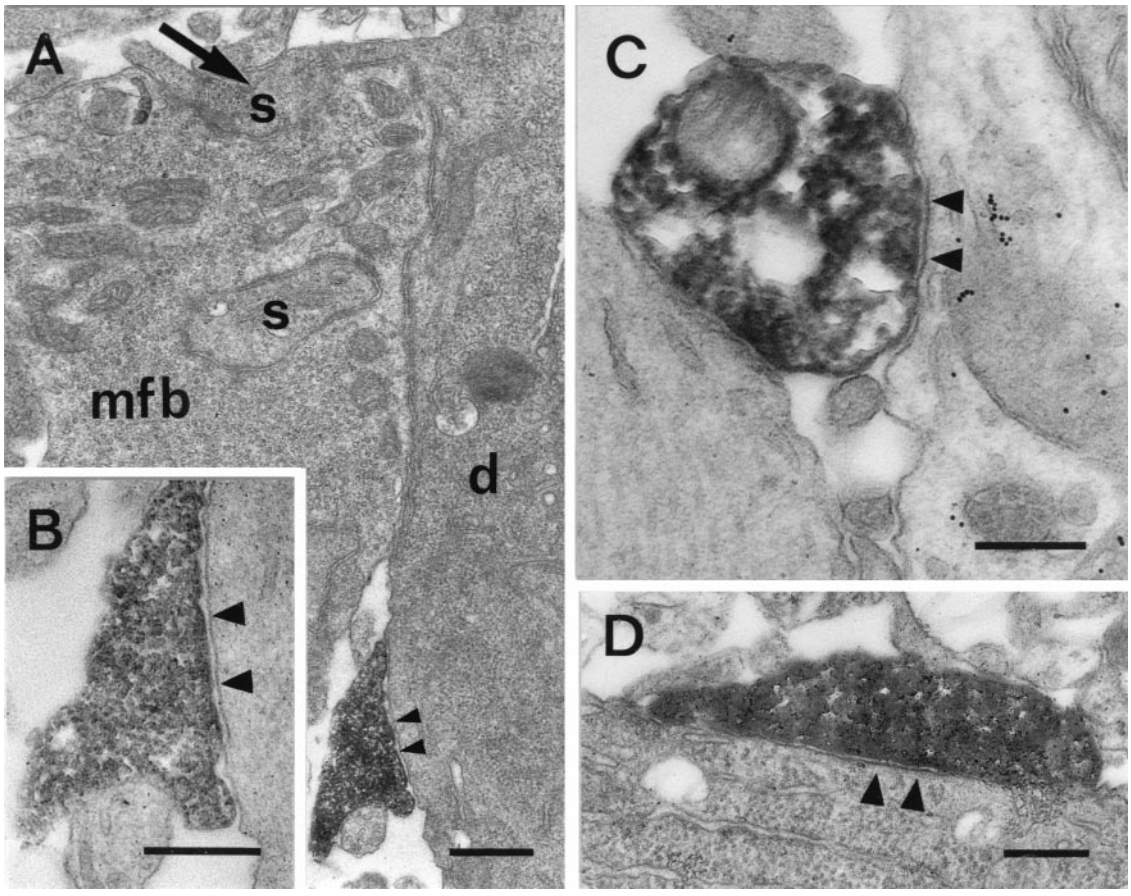

Fig. 2. Synapses formed by MFA interneurons in CA3. (*A*) Synaptic contact (◀) on a proximal apical dendritic shaft (d) made by a biocytin-filled bouton of an identified MFA interneuron. The dendrite was identified as belonging to a pyramidal cell by the large spines (s) establishing synaptic contacts with a mossy fiber bouton (mfb); one of the spines (arrow) is in direct connection with the dendritic shaft. (*B*) Higher magnification of the symmetric synaptic contact (◀) shown in *A*. (*C*) Biocytin-filled bouton of an MFA cell establishing symmetric synaptic contact (◀) with a spinefree, beaded dendrite. This dendrite most likely belongs to a GABAergic inhibitory neuron as indicated by the postembedding GABA immunogold labeling. (*D*) Symmetric synaptic contact (◀) formed by a biocytin-filled bouton on a cell body in the pyramidal layer of CA3. (Bars = (*A*) 0.5 μm; (*B*) 0.3 μm; and (*C* and *D*) 0.25 μm.)

neurons, as revealed by GABA postembedding immunostaining ($n = 5$ out of 26 tested; Fig. 2*C*). In the hilar region, synaptic contacts ($n = 5$; data not shown) were found on somata and proximal dendrites. Postembedding GABA immunostaining performed on adjacent sections showed that these postsynaptic neurons were not GABAergic and were therefore tentatively identified as mossy cells.

The postsynaptic targets of MFA interneurons included somata and proximal dendritic shafts similar to those of basket cells (12, 13, 28); however, the proportion of dendritic shafts among the targets of MFA interneurons was much higher. We made a statistical comparison of the target profiles of these two types by using the data of Halasy *et al.* (28) and found that MFA interneurons are significantly different from basket cells ($\chi^2 = 26.6; P < 0.01$), whereas the four MFA cells form a homogeneous sample ($\chi^2 = 0.2$).

To characterize the postsynaptic effect of these interneurons, we made recordings from synaptically coupled MFA interneurons and pyramidal cells ($n = 4$; Fig. 3). Postsynaptic currents had fast kinetics (Fig. 3 *Aa–Ac*) and were blocked by 10 μM bicuculline ($n = 2$ out of two tested; Fig. 3*Af*), indicating that they were $GABA_A$ receptor-mediated IPSCs. Unitary IPSCs had a short latency (1.7 ± 0.6 ms) consistent with the monosynaptic nature of the responses. Average IPSCs (Fig. 3*Ac*) had a mean rise time of 280 ± 80 μs (20–80%) and a half duration of 3.6 ± 1.3 ms. The decay of IPSCs could be fitted with a single exponential (Fig. 3*Ac*); the mean value of decay time constants was 4.6 ± 1.2 ms. The average amplitude of the IPSCs (excluding failures) ranged between 84 and 724 pA at a membrane potential of −70 mV with a mean value of 284 pA. In all pairs, individual IPSCs showed a 2- to 15-fold variation in amplitude (Fig. 3*Ab*). The proportion of failures varied between 3 and 55%. IPSCs elicited by trains of APs (8–10 delivered at 100–125 Hz) showed an approximately constant amplitude (measured from the baseline) during the train (Fig. 3 *Ad* and *Ae*).

By using the light microscope, all postsynaptic neurons were identified as pyramidal cells. Putative synaptic contacts were found on shafts of apical dendrites and also on somata (Fig. 3 *B* and *C*). All synaptic contacts were found within a distance of 35 μm measured from the soma. The number of light microscopically estimated synaptic contacts ranged from 2–8 with a mean value of 4. These numbers, however, have most likely been underestimated because axon collaterals in close proximity of the postsynaptic neurons were often obscured by the opaque mass of their somata and dendrites. Therefore, in one of the pairs, the postsynaptic pyramidal cell was reembedded and cut serially for electron microscopical analysis. In this pair, the two putative synaptic contacts, identified by light microscopy on the apical dendrite and the soma (Fig. 3*C*), were confirmed by electron microscopy. One additional bouton was found forming a synaptic contact with the soma.

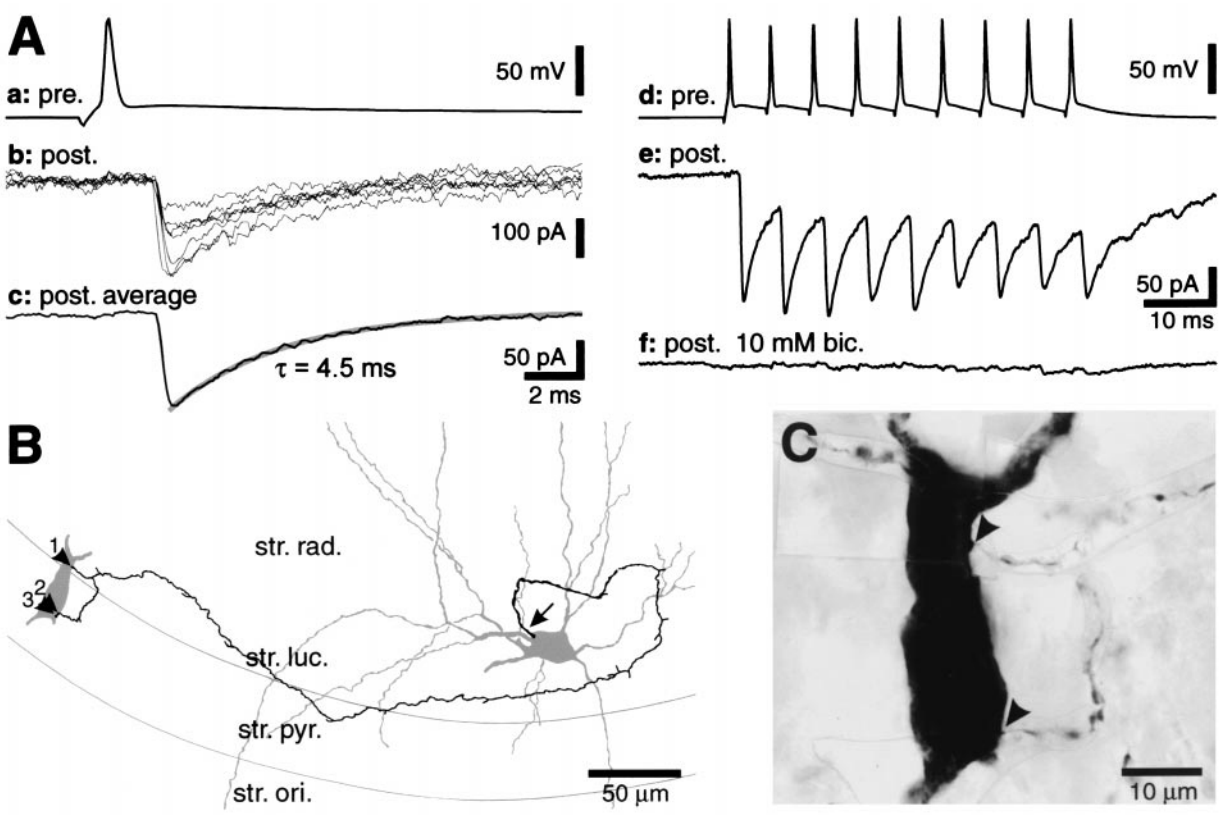

Fig. 3. Postsynaptic effect of an MFA interneuron on a morphologically identified CA3 pyramidal cell. (*A*) APs in the presynaptic interneuron (*Aa*) were followed by IPSCs of short latency in the postsynaptic pyramidal cell [(*Ab*) seven consecutive IPSCs superimposed; (*Ac*) average of 12 IPSCs; membrane potential −70 mV]. The decay phase of the average IPSC could be fitted with a single exponential with a time constant (τ) of 4.5 ms. During trains of APs (*Ad*), IPSCs showed a constant peak amplitude in the averaged response ($n = 26$, *Ae*). Bath perfusion of bicuculline (bic., 10 μM) blocked the synaptic response (*Af*, average of 25 traces, between 1.5 and 3 min of drug wash-in). (*B*) Camera lucida reconstruction of the presynaptic MFA interneuron (on the right) and the postsynaptic pyramidal cell (soma and proximal dendrites depicted only) with the route of the axon to the boutons forming the synaptic contacts. For clarity, only this part of the axonal plexus is illustrated. The arrow points to the axon initial segment; arrowheads indicate the boutons (1–3) forming synaptic contacts with the pyramidal cell. Bouton 3 was not observed in the light microscope but was found in the electron microscope when analyzing the serial thin sections. (*C*) Photomontage of the section containing the soma of the biocytin-filled postsynaptic pyramidal cell. The synaptic contacts identified in the light microscope are indicated by arrowheads. str. ori., stratum oriens; str. pyr., stratum pyramidale; str. luc., stratum lucidum; and str. rad., stratum radiatum.

Discussion

The present paper describes MFA interneurons of the hippocampal CA3 region. Physiological and morphological characteristics, and ultimately their GABAergic postsynaptic action, place MFA neurons in the heterogeneous class of inhibitory interneurons of the hippocampus (10). The distribution of the axon, however, does not correspond to that of any type of interneuron described so far, and it was used to identify these interneurons. In their intrinsic physiological properties, MFA neurons are homogeneous and show characteristics of interneurons such as brief APs and marked AHPs. Nevertheless, MFA interneurons cannot be identified solely on the basis of intrinsic properties, because the majority of nonpyramidal cells of the dendritic layers of CA1 and CA3 show similar characteristics (refs. 20, 25, and 26, and present results).

MFA interneurons have extensive local axonal arbors primarily located in the stratum lucidum, but they often extend into the hilar region. A neuron with a similar, but only partially recovered, axon was described in the guinea pig by Gulyás *et al.* (12). The authors classified this neuron as an atypical basket cell. Indeed, the postsynaptic elements of MFA interneurons include somata and proximal dendritic shafts similar to basket cells (12, 13, 28). However, quantitatively, the majority of synapses are formed on apical dendritic shafts. In statistical comparison, the two interneuron populations are significantly different in their postsynaptic target profiles. The output of MFA interneurons is directed to both principal cells and GABAergic interneurons. Nevertheless, the proportion of postsynaptic GABAergic cells is low, comparable to their low occurrence in the neuronal population. Although some types of interneurons exclusively contact other GABAergic neurons, thereby causing disinhibition of the principal cell population (10), most types target both pyramidal cells and interneurons with no preference (10, 29). The net effect of the latter (including MFA interneurons) is more likely to be a general reduction in the activity of the target cell population. Interconnections between GABAergic neurons are thought to be important in the generation of rhythmic population activity patterns, such as *theta* and *gamma* oscillations (30, 31).

MFA interneurons release GABA and activate $GABA_A$ receptors postsynaptically, similar to other types of interneurons (13, 25, 32). The postsynaptic effect is mediated by several synaptic contacts. The light microscopic estimate of four synaptic contacts per target cell is likely to be an underestimate for our sample of postsynaptic cells. Nevertheless, it is comparable to the number of contacts formed by interneurons mediating dendritic inhibition (13, 22, 25). From this number, we estimate that 1,300–1,700 postsynaptic neurons are contacted within a slice, indicating a divergence somewhat higher than that of basket cells (13, 28).

The majority of the excitatory synaptic inputs to MFA interneurons is likely to arise from the pyramidal cells of the ipsi- and

contralateral CA3 regions as indicated by the preferential location of MFA interneuron dendrites in the stratum radiatum and oriens. Whereas these interneurons most conceivably do not get significant input from the perforant path, they most likely receive input from the mossy fibers on their proximal dendrites located in the stratum lucidum (14, 33). In fact, in a recent study by Tóth and McBain (34), interneurons of the stratum lucidum were shown to receive synaptic input from both the commissural/associational pathway and the mossy fibers.

The axons of MFA interneurons terminate in conjunction with the mossy fibers as observed at both light and electron microscopic levels. The coalignment of the axon of inhibitory interneurons and afferent pathways is a general pattern in the hippocampus. It was first described for the dentate gyrus (11) and was later demonstrated in the CA1 and CA3 areas as well (12, 13, 15, 22, 25). Concerning the functional relevance of the coalignment of inhibitory and excitatory axons, one is tempted to speculate that this spatial association exists to facilitate interaction between the two. Dendritic inhibitory postsynaptic potentials may by local action efficiently control the integration of the afferent excitatory postsynaptic potentials (35, 36). In this context, it is interesting to note the fast kinetics of unitary IPSCs elicited by MFA interneurons. The decay of these IPSCs is considerably faster than that of perisomatic inhibitory currents in CA1 pyramidal cells (31, 37) and it is also faster than the decay of basket cell IPSCs recorded in granule cells in the dentate gyrus (38). These fast inhibitory synapses are located in the zone of the mossy fibers synapses where transmission is mediated by the AMPA/kainate-type of glutamate receptors; *N*-methyl-D-aspartate receptors have no or only a minor contribution (39).

The presence of $GABA_B$ receptors on afferent fibers raises the possibility that interaction might already take place at the presynaptic level. There is evidence that GABA released from an unidentified population of interneurons can reduce synaptic transmission at excitatory afferent pathways in the CA1 area via presynaptic $GABA_B$ receptors (24). The depression of synaptic transmission at the mossy fiber input to the CA3 region by synaptically released GABA has recently been demonstrated by Vogt and Nicoll (40). The density of axon collaterals of MFA interneurons and the actual proximity of their terminals to the mossy fiber boutons (Fig. 2*A*) suggest that MFA interneurons are the prime source of GABA spillover at the mossy fiber pathway.

Suppression of the mossy fiber pathway may play important roles in mnemonic processes. Several theories of hippocampal function suggest that the CA3 region serves to store associations of neural representations (4, 5, 8, 9). During the formation of associations (encoding), the activity of the CA3 region is "clamped" to the mossy fiber input (8, 9). Heterosynaptic inhibition during encoding may enhance the signal-to-noise ratio in the mossy fiber pathway (40). During retrieval of the associations, the mossy fiber input should be suppressed to avoid interference (5, 9). It has been suggested that this could be achieved by a reduction in the activity of the dentate gyrus itself (9). We propose that the recall process may be controlled by MFA interneurons. When activated, these interneurons may selectively suppress the mossy fiber input and thus enable the recall of information from the CA3 circuit.

We thank Drs. P. Jonas, E. H. Buhl, J. Lübke, and A. Woods for reading and commenting on an earlier version of the manuscript. I.V. would also like to thank J. Lübke for his help with the initial patch-clamp experiments and Dr. J. R. P. Geiger for stimulating discussions. The excellent technical assistance of S. Nestel, B. Joch, and K. Mews and photographic assistance of M. Winter and R. Hertweck are also gratefully acknowledged. This work was supported by the Deutsche Forschungsgemeinschaft (SFB 505).

1. Scoville, W. B. & Milner, B. (1957) *J. Neurol. Neurosurg. Psychiatry* **20,** 11–21.
2. Milner, B., Squire, L. R. & Kandel, E. R. (1998) *Neuron* **20,** 445–468.
3. Marr, D. (1971) *Philos. Trans. R. Soc. London B* **262,** 23–81.
4. Buzsáki, G. (1989) *Neuroscience* **31,** 551–570.
5. McClelland, J. L. & Goddard, N. H. (1996) *Hippocampus* **6,** 654–665.
6. Ishizuka, N., Weber, J. & Amaral, D. G. (1990) *J. Comp. Neurol.* **295,** 580–623.
7. Hopfield, J. J. (1982) *Proc. Natl. Acad. Sci. USA* **79,** 2554–2558.
8. McNaughton, B. L. & Morris, R. G. (1987) *Trends Neurosci.* **10,** 408–415.
9. Treves, A. & Rolls, E. T. (1992) *Hippocampus* **2,** 189–199.
10. Freund, T. F. & Buzsáki, G. (1996) *Hippocampus* **6,** 347–470.
11. Han, Z. S., Buhl, E. H., Lörinczi, Z. & Somogyi, P. (1993) *Eur. J. Neurosci.* **5,** 395–410.
12. Gulyás, A. I., Miles, R., Hájos, N. & Freund, T. F. (1993) *Eur. J. Neurosci.* **5,** 1729–1751.
13. Buhl, E. H., Halasy, K. & Somogyi, P. (1994) *Nature (London)* **368,** 823–828.
14. Frotscher, M., Soriano, E. & Misgeld, U. (1994) *Synapse* **16,** 148–160.
15. McBain, C. J., DiChiara, T. J. & Kauer, J. A. (1994) *J. Neurosci.* **14,** 4433–4445.
16. Paulsen, O. & Moser, E. I. (1998) *Trends Neurosci.* **21,** 273–278.
17. Gao, B. & Fritschy, J. M. (1994) *Eur. J. Neurosci.* **6,** 837–853.
18. Poncer, J. C., McKinney, R. A., Gähwiler, B. H. & Thompson, S. M. (1997) *Neuron* **18,** 463–472.
19. Martina, M., Schultz, J. H., Ehmke, H., Monyer, H. & Jonas, P. (1998) *J. Neurosci.* **18,** 8111–8125.
20. Kawaguchi, Y. & Hama, K. (1988) *Exp. Brain Res.* **72,** 494–502.
21. Cobb, S. R., Buhl, E. H., Halasy, K., Paulsen, O. & Somogyi, P. (1995) *Nature (London)* **378,** 75–78.
22. Miles, R., Tóth, K., Gulyás, A. I., Hájos, N. & Freund, T. F. (1996) *Neuron* **16,** 815–823.
23. Tsubokawa, H. & Ross, W. N. (1996) *J. Neurophysiol.* **76,** 2896–2906.
24. Isaacson, J. S., Solis, J. M. & Nicoll, R. A. (1993) *Neuron* **10,** 165–175.
25. Vida, I., Halasy, K., Szinyei, C., Somogyi, P. & Buhl, E. H. (1998) *J. Physiol. (London)* **506,** 755–773.
26. Spruston, N., Lübke, J. & Frotscher, M. (1997) *J. Comp. Neurol.* **385,** 427–440.
27. Somogyi, P. & Hodgson, A. J. (1985) *J. Histochem. Cytochem.* **33,** 249–257.
28. Halasy, K., Buhl, E. H., Lörinczi, Z., Tamás, G. & Somogyi, P. (1996) *Hippocampus* **6,** 306–329.
29. Cobb, S. R., Halasy, K., Vida, I., Nyiri, G., Tamás, G., Buhl, E. H. & Somogyi, P. (1997) *Neuroscience* **79,** 629–648.
30. Buzsáki, G. & Chrobak, J. J. (1995) *Curr. Opin. Neurobiol.* **5,** 504–510.
31. Whittington, M. A., Traub, R. D. & Jefferys, J. G. (1995) *Nature (London)* **373,** 612–615.
32. Miles, R. (1990) *J. Physiol. (London)* **431,** 659–676.
33. Acsády, L., Kamondi, A., Sík, A., Freund, T. & Buzsáki, G. (1998) *J. Neurosci.* **18,** 3386–3403.
34. Tóth, K. & McBain, C. J. (1998) *Nat. Neurosci.* **1,** 572–578.
35. Softky, W. (1994) *Neuroscience* **58,** 13–41.
36. Holmes, W. R. & Levy, W. B. (1997) *J. Neurophysiol.* **78,** 103–116.
37. Banks, M. I., Li, T. B. & Pearce, R. A. (1998) *J. Neurosci.* **18,** 1305–1317.
38. Geiger, J. R. P., Lübke, J., Roth, A., Frotscher, M. & Jonas, P. (1997) *Neuron* **18,** 1009–1023.
39. Jonas, P., Major, G. & Sakmann, B. (1993) *J. Physiol. (London)* **472,** 615–663.
40. Vogt, K. E. & Nicoll, R. A. (1999) *Proc. Natl. Acad. Sci. USA* **96,** 1118–1122.